Vol. 565: 79–93, 2017
doi: 10.3354/meps12009

MARINE ECOLOGY PROGRESS SERIES
Mar Ecol Prog Ser

Published February 17

Temporal genetic change in North American Pacific oyster populations suggests caution in seascape genetics analyses of high gene-flow species

Xiujun Sun[1,2], Dennis Hedgecock[1,*]

[1]Department of Biological Sciences, University of Southern California, Los Angeles, California 90089-0371, USA
[2]Yellow Sea Fisheries Research Institute, Chinese Academy of Fishery Sciences, Qingdao 266071, PR China

ABSTRACT: The Pacific oyster *Crassostrea gigas* was, for decades, massively introduced to North America from Japan and established large, self-recruiting populations in the Pacific Northwest of the USA and Canada. A previous study of mtDNA variation revealed little population genetic structure among populations from British Columbia and Washington State. Here, we used samples from that study, more recent samples from 2 of the same localities, and 2 additional samples, including 1 from Japan, to investigate spatial and temporal genetic variation at 52 mapped, coding, single-nucleotide polymorphisms (SNPs) assayed by high-resolution melting (HRM). Little variation was detected among North American populations, which, as a group, are distinct, perhaps adaptively so, from oysters in Hiroshima, Japan. However, significant excesses of heterozygotes with respect to random mating expectations and of pairwise linkage disequilibria revealed that North American populations are not in Hardy-Weinberg (random mating) equilibrium. Moreover, genetic changes over 10 to 21 yr in 2 localities are substantial, despite high gene flow, and are as large as spatial variance per generation. These results caution against basing connectivity or seascape genetic analyses on snapshots of spatial population structure in high gene-flow species. Because migration and selection are ruled out as causes of temporal genetic change, random genetic drift is the most parsimonious explanation. This implies effective population sizes (N_e) of hundreds to a few thousands, orders of magnitude smaller than the natural abundance (N) of this oyster. These low N_e:N ratios are compatible with the hypothesis of sweepstakes reproductive success.

KEY WORDS: *Crassostrea gigas* · Single nucleotide polymorphism · High-resolution melting · Linkage disequilibrium · Genetic variance · Effective population size · Sweepstakes reproductive success

INTRODUCTION

The impact of environmental, geographic, or historical factors on the genetic diversity of natural populations is a longstanding focus of population genetics. New vigor was brought to this field by landscape genetics, a fusion of landscape ecology and population genetics, which seeks insights mainly through spatial correlation of population genetic structure with demographic, geographic, and environmental parameters (Manel et al. 2003, Manel & Holderegger 2013). 'Seascape genetics' soon followed, with an early focus on quantifying connectivity of marine populations, often by correlating genetic distance with oceanographic distance among populations (reviewed by Riginos & Liggins 2013, Selkoe et al. 2016). Seascape genetics studies have more recently incorporated large oceanographic data sets and spatial autocorrelation to tease apart oceanographic from environmental de-

*Corresponding author: dhedge@usc.edu

terminants of spatial genetic structure and local adaptation (Selkoe et al. 2016).

Seascape genetics expanded upon earlier efforts to understand demographic connectivity of marine populations (Cowen & Sponaugle 2009). Population genetics has been central to connectivity research (Hedgecock et al. 2007a, Hauser & Carvalho 2008), owing to the theoretical equilibrium relationship, $F_{ST} = 1 / (4Nm + 1)$ (Wright 1931), in which genetic divergence among populations, quantified by Wright's standardized variance of allele frequencies among subpopulations, F_{ST}, or by similar measures (Hedrick 2005), is inversely proportional to the absolute number of migrants exchanged per generation, Nm, the product of population size, N, and migration rate, m. In contrast to the appealing simplicity of this theory, inference of Nm from F_{ST} in actual populations is fraught with statistical issues and with assumptions that are unlikely to be satisfied in nature (Whitlock & McCauley 1999). These key assumptions were often uncritically accepted or unappreciated in early connectivity research with high gene-flow marine species (Waples 1998, Hedgecock et al. 2007a) and in related research correlating F_{ST} and pelagic larval duration (see Faurby & Barber 2012).

'The two key steps of landscape genetics are the detection of genetic discontinuities and the correlation of these discontinuities with landscape and environmental features, such as barriers (e.g. mountains, gradient of humidity)' (Manel et al. 2003, p. 190). In landscape (or seascape) genetics, then, fine-scale spatial and temporal analyses reveal how environmental features (the independent variables) interact with microevolutionary processes (mutation, random genetic drift, migration, and selection) to shape population genetic structure (the dependent variable). Generally, spatial correlation of these independent and dependent variables assumes that microevolutionary forces—mainly migration, genetic drift of selectively neutral genetic markers, and selection—are near or have reached equilibrium, resulting in temporally stable population genetic structure (Manel & Holderegger 2013). Temporal landscape change, particularly anthropogenic perturbations, require methods that do not depend on migration-drift equilibrium, such as parentage assignment, and on critical attention to the scale of sampling, frequency of environmental data, and type and number of genetic markers (Manel & Holdregger 2013). Still, the seascape genetics literature has thus far been dominated by link- or node-levels of analysis (sensu Wagner & Fortin 2013) that depend on assumptions of Hardy-Weinberg (random mating) and migration-drift equilibria (Riginos & Liggins 2013, Selkoe et al. 2016). Unfortunately, equilibrium among microevolutionary forces is only rarely tested in seascape genetics studies, despite substantial evidence that it often does not hold for high gene-flow marine species (Hedgecock et al. 2007a, Hauser & Carvalho 2008). Temporal change, in particular, has been observed in several marine species, often giving rise to surprisingly low ratios of effective to census population numbers, N_e:N, the magnitudes and causes of which are debated (Hedgecock & Pudovkin 2011).

In the present study, we examine genetic diversity within and among populations of the Pacific oyster *Crassostrea gigas*, which was first introduced to western North America nearly a century ago, was sustained thereafter by decades of massive seed imports, and was naturalized long ago (Mann 1979, Quayle 1988). The history of this population suggests the absence of either a founder effect or admixture of genetically differentiated stocks (Supplement 1, 'History of US Pacific oyster populations', at www.int-res.com/articles/suppl/m565p079_supp1.pdf). We used samples from previous studies of these oyster populations (Boom et al. 1994, Langdon et al. 2003), together with more recent samples from 2 of the same localities and a sample from Japan, to describe genetic diversity on local as well as broad spatial and temporal scales.

Using single nucleotide polymorphisms (SNPs) and traditional population genetics approaches, we tested Hardy-Weinberg equilibria, for individual loci and pairwise combinations, within local population samples, and we measured temporal change at 2 sites. We estimated effective population size, N_e, from measures of linkage disequilibrium (Do et al. 2014) and temporal genetic change (Nei & Tajima 1981, Pollak 1983, Waples 1989, Wang 2001) and examined the assumptions of no migration or selection critical to the interpretation of results.

MATERIALS AND METHODS

Biological material

In total, 553 individuals were obtained from 10 spatial and temporal samples of Pacific oysters from North America and Japan (Table 1). Four of these samples were from British Columbia (BC), Canada (Pendrell Sound, Hotham Sound, Hisnit Inlet, and Pipestem Inlet), 2 were from Washington State, USA (Dabob Bay and Willapa Bay), and 1 was from Hiroshima, Japan (Fig. 1). Temporal samples were

Table 1. Location, sample code, collection year, and sample sizes for all populations of Pacific oyster *Crassostrea gigas*

Location	Sample code	Year	Sample size
Pendrell Sound, Canada	Pend90	1990	23
Hotham Sound, Canada	Hoth90	1990	24
Hisnit Inlet, Canada	Hisn90	1990	24
Pipestem Inlet, Canada	Pipe90	1990	22
Pipestem Inlet, Canada	Pipe10	2010	148
Dabob Bay, USA	Dab85	1985	16
Dabob Bay, USA	Dab96	1996	94
Dabob Bay, USA	Dab06	2006	92
Willapa Bay, USA	Will96	1996	30
Hiroshima, Japan	Hiro96	1996	80

collected from Dabob Bay (1985, 1996, and 2006) and Pipestem Inlet (1990 and 2010). Samples from Pendrell Sound, Hotham Sound, Hisnit Inlet, Pipestem Inlet (1990), and Dabob Bay (1985) were the same as those analyzed for mtDNA variation by Boom et al. (1994); although year of collection is not given in their paper, the Dabob Bay sample, which was provided by one of us (D.H.), was collected in 1985, and the rest were likely collected in 1990, when funding for the project began (A. T. Beckenbach pers. comm.). The 1996 samples from Dabob and Willapa Bays were collected to initiate a selective breeding program (Langdon et al. 2003). Samples comprised mixed-age adults, except for the 1985 sample from Dabob Bay, which was a collection of young-of-the-year juveniles. Analysis of spatial variation was made with the BC samples and the 1996 collections from Dabob and Willapa Bays and Hiroshima.

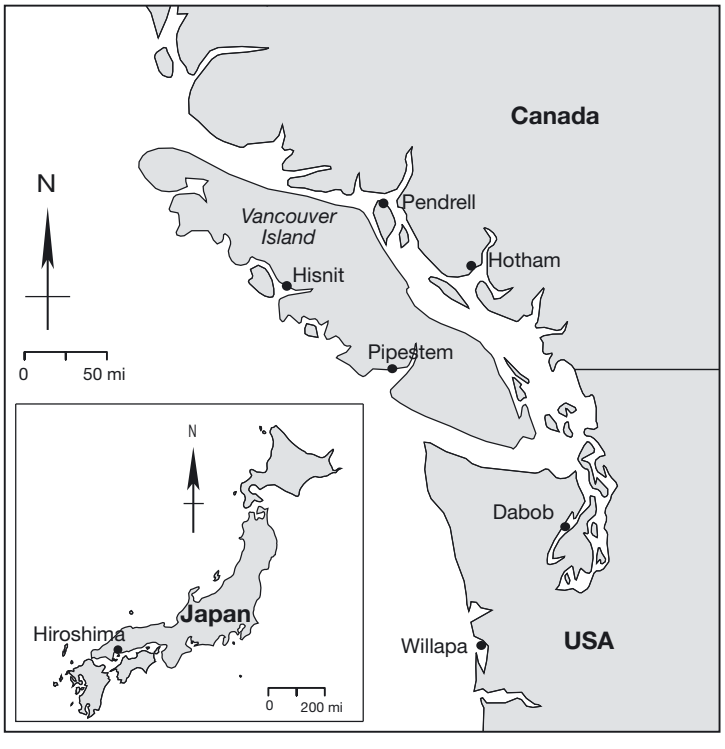

Fig. 1. Sample locations for Pacific oyster *Crassostrea gigas* in North America and Japan

Molecular methods

Genomic DNA was extracted from muscle samples of oysters using the Qiagen DNeasy kit according to the manufacturer's standard protocol. DNA concentration was determined by Quant-iT PicoGreen dsDNA Reagent and Kits (Invitrogen) and normalized to 5 ng μl^{-1} for each sample. High-resolution melting (HRM) assays for target SNPs in 52 coding sequences were developed by Sun et al. (2015), from the >1100 SNPs identified in expressed sequence libraries and placed on Pacific oyster linkage maps (Hedgecock et al. 2015). Hedgecock et al. (2015) focused on coding sequences to reduce the probability, in this extremely polymorphic species (Zhang et al. 2012), that nearby SNPs would interfere with the typing of target SNPs or give rise to null alleles, as commonly encountered in microsatellite DNA markers (Hedgecock et al. 2004). Since coding sequences are more likely to be under natural selection than non-coding sequences, we applied several tests for selection, as described below.

HRM assays were performed using 96-well or 384-well plates, each in a final volume of 10 µl containing 5 ng of genomic DNA, 0.175 µmol of each primer, 5 µl LightCycler 480 HRM Master Mix (Roche), and 3 or 3.5 mmol $MgCl_2$. Subsequent amplification of target amplicons was carried out on a LightCycler 480 System (Roche Diagnostics), under the following conditions (Sun et al. 2015): 10 min at 95°C followed by 40 to 45 cycles of amplification, each including 10 s of denaturation at 95°C, 10 s of annealing at 57–62°C, and 5 s extension at 72°C. After PCR amplification, products were immediately heated to 95°C for 1 min and then cooled to 40°C, followed by a continuous temperature increase of 0.05°C s^{-1} to a target temperature of 95°C. During the entire heating process, fluorescence was monitored from each well, and genotypes were determined by examining the normalized melting curves, using Light-

Cycler 480 Software (Roche). These melting curves are phenotypes, the genetic bases of which have been established through formal genetic analyses (Hedgecock et al. 2015, Sun et al. 2015).

Most HRM phenotypes are 'canonical,' reflecting simple SNP variation at the target sites (e.g. genotypes A/A, G/G, A/G or A/A, C/C, A/C), but a minority is 'non-canonical,' i.e. more complex HRM phenotypes arising from additional SNPs in the target amplicon (e.g. A/X, A/Y, A/Z, C/X, C/Y, G/X, G/Y, G/Z, X/X, Y/Y, and Z/Z, in which X, Y, and Z are sequences differing from the corresponding canonical exon sequence at up to 4 sites besides the target SNP). These non-canonical HRM phenotypes are testament to the extremely high polymorphism of the Pacific oyster; having determined their genetic basis, however, Sun et al. (2015) showed that non-canonical HRM markers have higher allelic diversity than simple bi-allelic SNPs. HRM genotyping also has high accuracy; Sun et al. (2015) detected only 1 inconsistency out of 449 duplicate PCR-HRM assays for 50 markers across 9 individuals (1 instance of missing data), a genotyping error rate of 0.22%.

Genetic variation within and among population samples

Standard population genetic statistics, viz. the observed number of alleles per locus, observed (H_o) and expected proportions of heterozygotes per locus (H_e; H_{nb}, non-biased; Nei 1978), and the inbreeding coefficient F_{IS} (Weir & Cockerham 1984), were used to describe genetic variability within population samples. These genetic parameters were computed for each locus and population using the Genetix 4.05 software package (Belkhir et al. 2004). The significance of F_{IS} was determined for each locus and population, using the web version of Genepop 4.2 (Raymond & Rousset 1995, http://genepop.curtin.edu.au/), which implements a Markov chain method, with 1000 dememorization steps, 100 batches, and 1000 iterations per batch. Tests for linkage disequilibrium (LD) among pairs of loci were performed using Genepop software 4.1.3 (Rousset 2008) and Genetix 4.05, which permits partitioning of variance in LD into within- and among-population components (Ohta 1982). The extent of population differentiation was quantified using conventional F_{ST} values, which were tested for significant departure from 0 using 10 000 permutations, as implemented in the program Genetix 4.05. Corrections of the significance level for multiple tests were carried out following the Bonferroni procedure (Rice 1989). Genetic relationships were also examined using the covariance-standardized principal coordinates analysis (PCoA) method in GenAlEx 6.5 to detect and visualize pairwise Nei's genetic distances among populations (Peakall & Smouse 2012). To compare allelic richness among populations, we used FSTAT 2.9.3 (updated from Goudet 1995) to estimate the expected number of alleles per locus in a sample size of 16 diploid individuals (the smallest sample size for this study). SNP genotypes and genotypes recoded for Genetix or Genepop are provided in Supplement 2 at www.int-res.com/articles/suppl/m565p079_supp2.xlsx.

Temporal variance in allelic frequencies

Analysis of temporal variance was done in 2 populations, Dabob Bay and Pipestem Inlet, which are represented by 3 and 2 temporal samples, respectively. The number of generations between samples was calculated assuming 2 or 2.5 yr per generation in Dabob Bay and 2 or 3 yr in Pipestem Inlet, where mean generation time might be longer owing to colder waters and less harvest pressure (i.e. less of a collapsed age structure). Of the available estimators of standardized temporal variance in allele frequency (Nei & Tajima 1981, Pollak 1983, Jorde & Ryman 2007), we chose the Jorde and Ryman F_s estimator, because it is the least sensitive to rare alleles and overcomes bias in cases of small sample size. We note here that F_s between 2 populations (1 and 2) is expected to be twice as large as the F_{ST} calculated from the same allele-frequency data, since $F_s \propto (x_1 - x_2)^2$, while $F_{ST} \propto \sum_{i=1}^{2} (x_i - \bar{x})^2$.

Estimation of effective population sizes (N_e) and migration rates

Single-sample and temporal methods were used to estimate N_e, using NeEstimator v2.0 (Do et al. 2014). The single-sample, linkage-disequilibrium, LDNe estimator (based on the mean squared correlation of allele frequencies at different loci, r^2, rather than the measure, D; Waples & Do 2008) was used to estimate N_e for all populations, while the single-sample, heterozygote excess (Zhdanova & Pudovkin 2008) and molecular co-ancestry methods (Nomura 2008) were used only for the Dab85 sample, which represents a cohort of juveniles settled in that year. For both single-sample analyses and temporal comparisons, we set minimum allele frequency thresholds (P_{crit}) so as

to eliminate bias from singleton alleles (Do et al. 2014).

We used NeEstimator to estimate N_e based on F_s estimates of allele-frequency variance over time intervals with plan II sampling (i.e. sampling before reproduction without replacement; Waples 1989). We also used a pseudo-likelihood method to estimate N_e for temporal intervals in the Pipestem Inlet and Dabob Bay populations, assuming no migration and the largest maximum prior population size for the available computer RAM (35 750; Wang 2001). In addition, we jointly estimated N_e and m, the migration rate (Wang & Whitlock 2003), for each of these focal populations, using a pool of the 5 remaining North American populations sampled in 1990 or 1996 to represent an infinite source of immigrants. We rounded numbers of generations estimated for the various temporal intervals to the nearest integer but did not apply the recommended corrections of the resulting estimators back to non-integer intervals, as these were very small. Finally, we did not assume that the focal and source populations were in migration-drift equilibrium. Analyses were done with MLNe, which provides maximum likelihood (ML) estimates and 95% confidence intervals as well as moment estimates (MT_N_e and MT_m but no confidence intervals for these; Wang & Whitlock 2003). We note that a recent evaluation of methods for estimating N_e, with and without migration, showed that the primary methods used here — the Jorde & Ryman (2007) estimator, the moment and maximum likelihood temporal methods (MLNe; Wang & Whitlock 2003), and the LDNe method (Do et al. 2014) — all perform well over a range of simulated population demographics and sampling strategies, which include those in this study (Gilbert & Whitlock 2015). These methods have good power to detect small to moderate population sizes, with modest accuracy and precision.

Testing for selection

Since the 52 HRM markers are mapped (Hedgecock et al. 2015, Sun et al. 2015), we looked for evidence that divergence between the Japanese and North American populations is concentrated at certain genomic locations, as might be expected under selection. We also tested for significant outlier F_{ST} values in this same Japan–North America comparison and among North American populations, calculating pairwise F_{ST} in 20 000 coalescent simulations, using the hierarchical island model implemented in Arlequin version 3.5.1.3. The results were used to generate the joint distribution of F_{ST} versus heterozygosity for the observed loci. Loci significant at the 1% level were identified as outliers being putatively under selection.

For temporal genetic data, we used probability plots to see if distributions of $n\hat{F}/\bar{F}$ conform to χ^2 distribution with $n = 52$ degrees of freedom, which is the distribution expected under selectively neutral evolution by random genetic drift in an isolated population (Nei & Tajima 1981, Waples 1989). Since our samples are from populations that are likely exchanging genes, we used a SimuPOP (Peng & Kimmel 2005) to explore how a probability plot of $n\hat{F}/\bar{F}$ might depart from linearity under the influence of migration (details in Supplement 1).

RESULTS

Genetic diversity of HRM markers within populations

Melting profiles for 52 HRM markers were obtained from 553 individuals, derived from 10 spatial and temporal population samples from North America, with sample sizes ranging from 16 to 148 (Table 1). Of the 28 756 possible phenotypes (i.e. 553 individuals × 52 markers), 28 616 were scored, while only 140 could not be scored (0.5% of all possible phenotypes). The majority of HRM phenotypes (26 377, 91.7%) corresponded to the canonical phenotypes expected for variation at the target SNPs, while the minority (2239; 7.8%) comprised a variety of non-canonical HRM phenotypes, arising from additional, non-target SNPs in the amplicons (Sun et al. 2015). Non-canonical HRM melting profiles were observed at 48 of the 52 loci; as a result of detecting additional, non-target SNPs, the HRM markers had from 3 to 5 alleles. We detected a total of 184 different alleles, giving grand averages of 3.53 alleles locus^{-1} and 2.92 alleles locus^{-1} population^{-1}, the latter varying from 2.62 to 3.35 over population samples (Table 2).

Descriptive genetic statistics are given for each locus and population (see Table S5 in Supplement 1) and are summarized in Table 2. H_o was similar across populations, with a grand, weighted mean of 0.451; likewise, H_e and H_{nb} were similar across populations and had grand weighted means of 0.441 and 0.443, respectively. The grand mean of A_r, 2.62, was not significantly different among populations ($F_{9,510} = 0.656$, $p = 0.749$) and showed no secular trends across the 2 series of temporal samples.

Table 2. Summary statistics of variability at 52 high-resolution melting (HRM) markers in 10 populations of Pacific oyster *Crassostrea gigas*. Population sample codes as in Table 1. Statistics are as follows: $\bar{n}$: average number (±SD) of individuals assayed per locus; H_e, H_{nb}, and H_o: average (±SD) proportions of heterozygotes per loci expected under random mating, expected under random mating and corrected for sampling bias, and observed, respectively; F_{IS}: inbreeding coefficient, with probabilities determined by 10 000 permutations of alleles among individuals within each population; $P_{(0.95)/(0.99)}$: proportions of polymorphic loci, P, at which the most frequent allele does not exceed a frequency of 0.95 (0.99); $\bar{n}_a$: average number of alleles per locus; A_r: allelic richness per locus, at a minimum common sample size of 16 individuals

Population	$\bar{n}$	H_e	H_{nb}	H_o	F_{IS}	p	$P_{(0.95)}$	$P_{(0.99)}$	$\bar{n}_a$	A_r
Pend90	22.9 ± 0.3	0.415 ± 0.137	0.424 ± 0.140	0.407 ± 0.148	0.041	0.068	0.942	1.0	2.750	2.613
Hoth90	23.7 ± 0.5	0.430 ± 0.132	0.439 ± 0.135	0.434 ± 0.159	0.011	0.347	0.981	1.0	2.769	2.631
Hisn90	23.9 ± 0.2	0.438 ± 0.104	0.447 ± 0.106	0.475 ± 0.158	−0.064	0.007	1.0	1.0	2.692	2.581
Pipe90	21.7 ± 0.5	0.420 ± 0.136	0.430 ± 0.139	0.411 ± 0.150	0.045	0.053	0.962	1.0	2.615	2.460
Pipe10	147.2 ± 1.2	0.446 ± 0.103	0.448 ± 0.104	0.449 ± 0.118	−0.002	0.451	1.0	1.0	3.346	2.636
Dab85	16.0 ± 0.0	0.441 ± 0.130	0.456 ± 0.134	0.498 ± 0.204	−0.095	0.001	0.981	1.0	2.654	2.673
Dab96	93.7 ± 0.6	0.448 ± 0.112	0.450 ± 0.113	0.465 ± 0.130	−0.033	0.005	1.0	1.0	3.154	2.640
Dab06	91.8 ± 0.6	0.437 ± 0.109	0.439 ± 0.109	0.445 ± 0.123	−0.013	0.158	1.0	1.0	3.231	2.680
Will96	29.7 ± 0.6	0.434 ± 0.120	0.441 ± 0.122	0.447 ± 0.151	−0.014	0.272	0.981	1.0	2.865	2.666
Hiro96	79.7 ± 0.6	0.450 ± 0.104	0.453 ± 0.104	0.472 ± 0.130	−0.041	0.002	1.0	1.0	3.154	2.647

Average F_{IS} over all loci and populations was −0.021, indicating a small but significant ($p < 0.003$) excess of heterozygotes with respect to random mating proportions. Average F_{IS} values for populations were negative (heterozygote excess) in all but 3 samples and significantly negative in 4 samples. Over all loci and populations (520 tests), F_{IS} was significant at the nominal 5% level in 99 cases (19%); in 85 of these cases, F_{IS} was negative.

Significant levels of LD for pairs of markers were detected in all populations, except Hoth90. For 9 of the 10 populations, the number of LD values exceeding nominal significance was significantly greater than the 66 expected (5% of 1326 pairwise combinations), i.e. 101, 105, 86, 100, 101, 97, 87, 86, and 86, respectively. Average LD values for linked (n = 178) and unlinked pairs (n = 1148) of markers were not significantly different in 9 populations and had a borderline significant difference in Pend90 (Table S1 in Supplement 1). Five populations had average LD (measured by r^2) that exceeded the expectation based on sample size alone (Table 3); we used these 5 populations to illustrate the low overlap of high-LD combinations among populations. Of the 420 SNP pairs with significant LD in these 5 populations, 354 pairs (84.3%) were found in only 1 sample, 62 (14.7%) were shared by 2 samples, 4 (1%) were shared by 3 samples, and none was shared by 4 or 5 of these samples (Tables S2 & S3 in Supplement 1). The partitioning of LD variance (D_{IT}^2) into within (D'_{IS}^2) and among (D'_{ST}^2) population components, showed that 99% of LD variance was within, not among populations; the ratio of D'_{IS}^2 to D_{IT}^2 ranged from 0.864 to 1.0 across SNP pairs, with a mean of 0.987 and a median of 0.992.

Genetic diversity among spatial population samples

Among the 7 populations used for analysis of spatial variance, genetic differentiation was low but highly significant (global F_{ST} = 0.0099, $p < 0.0001$). Most of this variance, however, was between Hiro96 and North American populations, with F_{ST} values in pairwise comparisons ranging from 0.015 to 0.021 ($p < 0.0001$ in all cases; Table 4). Significant variance of allelic frequencies was found among the 6 North American populations (F_{ST} = 0.0027, $p < 0.020$), but when Pipe90 was removed, the remaining populations were homogeneous (F_{ST} = 0.001, $p > 0.05$). Pipe90 showed significant divergence only from Dab96 (p = 0.0003; Table 4, Fig. 1).

A plot of the first and second principal coordinates, accounting for 49.4 and 28.7% of total allele-frequency variation, respectively, gives a visual representation of genetic distance among the 10

Table 3. Mean sample sizes per locus ($\bar{n}$), mean squared correlation of allelic frequencies over all pairs of loci (r^2), the expectation of r^2 based on mean sample size ($E(r^2)$), and effective population sizes (N_e) for 5 Pacific oyster *Crassostrea gigas* populations (see Table 1) estimated by the linkage disequilibrium method

Population	$\bar{n}$	r^2	$E(r^2)$	N_e (95% CI)
Hisn90	23.9	0.050	0.048	118 (61–793)
Pipe90	21.4	0.058	0.054	70.7 (41.4–194.9)
Dab85	16.0	0.087	0.076	23.7 (17.0–36.5)
Dab96	93.4	0.012	0.011	279 (202–435)
Dab06	91.4	0.012	0.011	790 (396–12548)

population samples (Fig. 2). In accordance with the F_{ST} estimates, the Hiroshima population (Hiro96) was well differentiated from the North American populations. Temporal samples contributed substantially to the scatter of points; samples from Pipestem Inlet were widely separated on the second axis, while samples from Dabob Bay were equally separated on both axes.

Temporal variance in allele-frequencies

Allele-frequency variance between temporal samples was significantly greater than sampling variance (the inverse of average harmonic mean sample size per locus) in all comparisons within the Pipestem Inlet and Dabob Bay localities (Table 5). Between 1990 and 2010 in Pipestem Inlet, $F_s = 0.05$. For Dabob Bay, $F_s = 0.042$, 0.013, and 0.042 for the 1985 to 1996, 1996 to 2006, and 1985 to 2006 intervals, respectively. Dividing these temporal variances by 2, to put them on the same scale as spatial variance (see 'Materials and methods'), and by the number of generations in the interval measured (Table 5), to put them on a per generation basis, we see that temporal variance per generation is 0.5 to 1.4 times as large as spatial variance among North American populations ($F_{ST} = 0.0027$).

Estimation of effective population size, N_e, and joint estimates of N_e and migration rate

Estimates of N_e, using the single-sample LD method, were finite, with finite upper 95% confidence limits, for 5 populations (Table 3). Estimates of N_e ranged from 23.7 for Dab85 to 790 for Dab06. The effective number of breeders, N_b, for Dab85 was 8.4 and 7.8 by the heterozygote-excess and molecular-coancestry methods, respectively. N_e was expected to be larger than N_b for Dab85 because the LD estimate is the harmonic mean of N_b and N_e with overlapping generations (Waples et al. 2014).

Estimates of N_e based on temporal genetic variance and assuming isolation of the Pipestem Inlet and Dabob Bay populations ranged from 146 to 1188, all with finite upper 95% confidence limits (Table 5). Estimates and their confidence limits are not much affected by different assumptions of generation intervals; longer generation times mean fewer generations per interval, resulting in smaller effective population sizes, as expected.

Joint estimates of N_e and m suggest that migration rates were very high ($m > 0.14$; Table 5). Moment estimates of m, which lack confidence intervals, were smaller than corresponding maximum likelihood estimates, though still quite high ($0.11 < m < 0.45$). Taking the homogenizing effects of migration into account, ML estimates of N_e were considerably smaller than those estimated under the assumption of complete isolation, using either the MT or Jorde and Ryman estimators.

Testing for selection in spatial and temporal samples

Estimation of N_e depends critically on the assumption of no selection, which we examined on 2 levels. First, we investigated the large difference between

Table 4. Pairwise F_{ST} comparisons among the 7 Pacific oyster *Crassostrea gigas* populations (see Table 1). Values in **bold** are significant after adjusting the threshold by the sequential Bonferroni method (Rice 1989)

	Pend90	Hoth90	Hisn90	Pipe90	Dab96	Will96	Hiro96
Pend90	–	–0.0013	–0.0021	0.0063	0.0040	–0.0009	**0.0177**
Hoth90			–0.0009	0.0029	0.0006	0.0009	**0.0188**
Hisn90				0.0058	–0.0010	0.0027	**0.0194**
Pipe90					**0.0118**	0.0033	**0.0212**
Dab96						0.0020	**0.0153**
Will96							**0.0151**
Hiro96							–

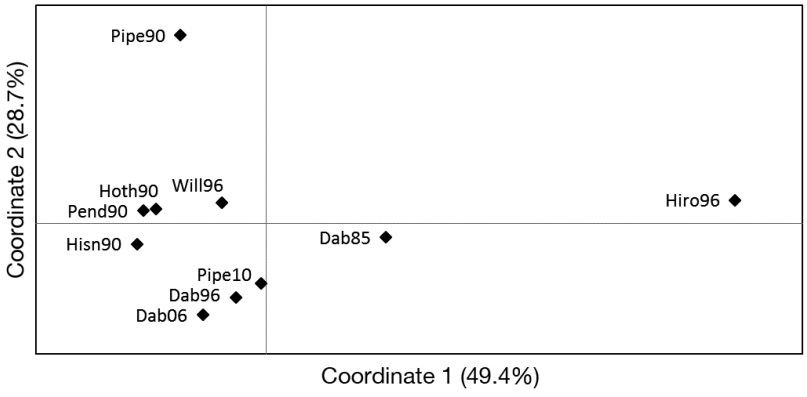

Fig. 2. Principal coordinates analysis of genetic similarity among 10 Pacific oyster *Crassostrea gigas* populations (see Table 1)

Table 5. Effective population sizes for 2 Pacific oyster *Crassostrea gigas* populations (see Table 1), estimated by the Jorde & Ryman (2007) estimator of temporal variance F_s and Wang's (2001) pseudo-likelihood method (MLNe), which simultaneously estimates migration rate. MT_Ne is the moment-based estimator of N_e, assuming no migration; MT_m is the moment-based estimator of migration, which has no confidence limits. Numbers of generations, rounded to the nearest integer for the maximum likelihood method (Wang & Whitlock 2003), are calculated assuming 2 or 2.5 yr for Dabob Bay and 2 or 3 yr for Pipestem Inlet. For joint estimates of N_e and m for Dabob Bay, the 1996 sample is taken as $t = 0$, contemporaneous with spatial samples in the source pool; populations are not assumed to be in migration-drift equilibrium at the start. CI: confidence interval

Population, interval	Number of generations	Harmonic mean sample	F_s	Estimated N_e (95% CI) From F_s	Estimated N_e (95% CI) From MLNe	MT_N_e	Estimated m (95% CI), from MLNe	MT_m
Dabob Bay								
Dab85/96	5.5, ~5	27.3	0.0417	585 (439–751)	8.8 (5.5–17)	571	0.49 (0.001–1.0)	0.30
Dab85/96	4.4, ~4	27.3	0.0417	468 (351–601)	8.8 (5.5–17)	457	0.14 (0.001–1.0)	0.36
Dab96/06	5.0	92.7	0.0129	1188 (913–1498)	295 (149–746)	526	0.14 (0.08–0.23)	0.11
Dab96/06	4.0	92.7	0.0129	950 (730–1198)	238 (123–590)	421	0.18 (0.11–0.28)	0.13
Dab85/06	10.5, ~10	27.2	0.0423	1011 (758–1299)	183 (97–437)	548	0.33 (0.25–0.50)	0.16
Dab85/06	8.4, ~8	27.2	0.0423	809 (607–1039)	160 (86–373)	438	0.40 (0.30–0.57)	0.20
Dab85/96/06	–5, 0, 5	—	—	—	133 (72–284)	—	0.35 (0.26–0.65)	0.20
Dab85/96/06	–4, 0, 4	—	—	—	115 (65–241)	—	0.42 (0.31–0.69)	0.24
Pipestem Inlet								
Pipe90/10	10	37.7	0.0498	219 (165–280)	135 (85–443)	324	0.99 (0.20–1.0)	0.35
Pipe90/10	6.7, ~7	37.7	0.0498	146 (111–187)	136 (85–374)	227	0.99 (0.27–1.0)	0.45

the Japanese and North American population samples for signals of selection that might have accumulated over decades of isolation. Since all North American populations, except Pipe90, are statistically homogeneous, we pooled these 5 samples for a more robust comparison between the North American and Japanese (Hiro96) populations. As the HRM markers are mapped (Table S6 in Supplement 1), we can examine the distribution of F_{ST} across the genome (Fig. 3A), which reveals that 3 markers make a disproportionate contribution to divergence. Two of the outliers, 1893-G130921T and 1893-T131175C, are in the same genome scaffold (1893) and are located on linkage group 1. The other outlier, 42684-C117024T, is on linkage group 8. Observed F_{ST} for the most divergent locus, 1893-G130921T, 0.122, is 7.5 times greater than the global F_{ST} of 0.0162.

An outlier analysis, using a hierarchical island model (Excoffier et al. 2009), supports this finding, indicating that these same 3 markers fell outside of the 99% confidence interval for the simulated distribution of F_{ST} against expected heterozygosity (Fig. 3B). Allele frequencies at these 3 markers differed conspicuously between North America and Japan (Fig. 3C). The remaining 49 markers appeared to have less divergence than expected between Japan and North America, as only 1 fell outside of the 10% quantiles in Fig. 3B, when 10 were expected; rerunning this analysis without the outliers produces similar results, with only 4 markers lying outside of the 10% quantiles (χ^2 goodness-of-fit, adjusted for continuity = 3.59; p = 0.058). When this analysis was repeated with just the 5 North American populations by themselves, no outliers were observed, suggesting an absence of strong diversifying selection among North American populations.

Next, we examined the temporal data for signs that selection has caused genetic change. In an isolated population undergoing random genetic drift, $n\hat{F}/\bar{F}$ should follow a chi-squared distribution with 52 degrees of freedom (see 'Materials and methods'). Probability plots of the transformed F_s values for Dabob Bay and Pipestem Inlet revealed a clear and characteristic difference from the chi-squared distribution (Fig. 4A). In both cases, ~35 markers fell well below expected values, meaning smaller-than-expected temporal change, while a group of ~12 markers rose well above expected values, meaning much larger-than-expected temporal change. Simulations of genetic drift in a small local population (N_e = 100), exchanging migrants with a larger metapopulation and having similar levels of genetic variability as the actual populations (Table S4 in Supplement 1), reproduced this characteristic pattern of departure from the chi-squared distribution (Fig. 4B; Fig. S1 in Supplement 1).

There was no correlation between the ranks of locus-specific F_s values in the Pipestem Inlet and Dabob Bay populations (p = 0.24; Fig. 5A). The 3 outliers in the Japan to North America comparison

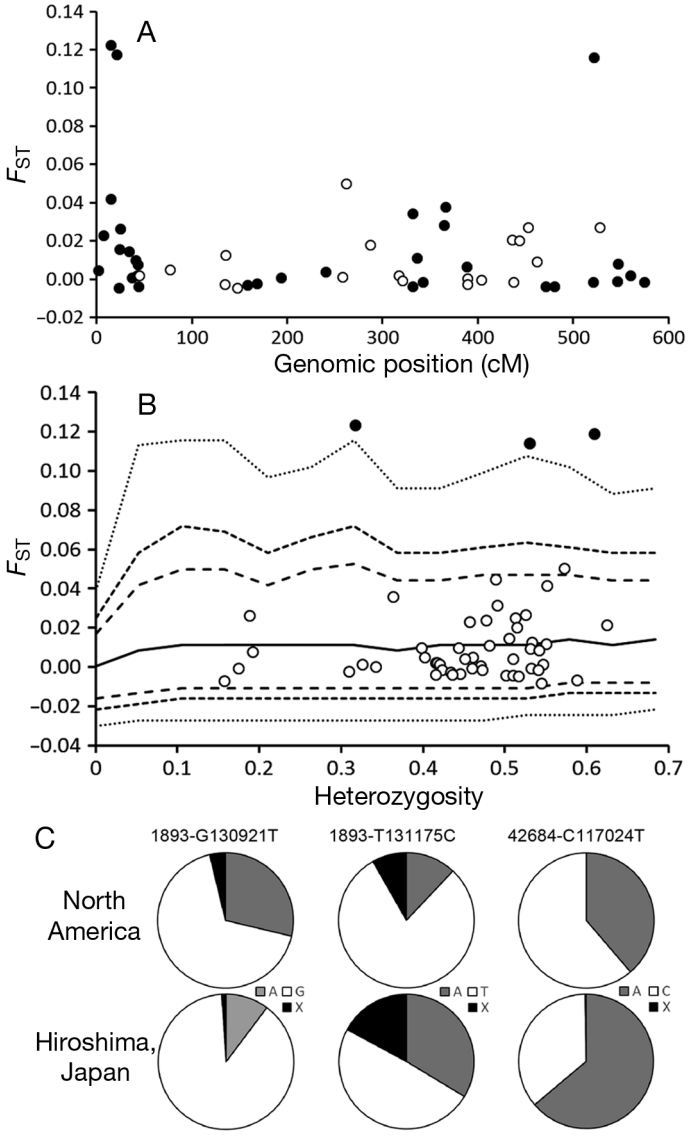

Fig. 3. Genetic divergence of North American and Japanese populations of Pacific oyster *Crassostrea gigas*. (A) F_{ST} for 52 single nucleotide polymorphisms (SNPs), between North American and Japanese populations, by genomic position; markers are alternately filled or unfilled to show the 9 linkage groups covered. (B) Distribution of F_{ST} at 52 SNPs, by heterozygosity; quantiles of 50, 10, 5, and 1%, obtained by simulation, are shown in solid (50%) and variously dashed lines. (C) Allele frequencies at 3 F_{ST}-outlier SNPs in North American and Japanese Pacific oyster populations; X is a non-canonical high-resolution melting (HRM) allele at each of the loci

are notably among those markers with smaller-than-expected change in both temporal series. For comparison, there was also no correlation in the ranks of locus-specific F_s values between two 10-generation intervals (90 to 100 and 110 to 120) in the simulated population (N_e = 100) undergoing random genetic drift with migration from a larger metapopulation (Fig. 5B).

DISCUSSION

Testing critical assumptions of seascape genetics

The Pacific oyster shows the slight but statistically significant differences in allele-frequencies typically observed among populations of marine species with dispersing, planktonic larvae (Hedgecock et al. 2007a, Hauser & Carvalho 2008). Most of the variance in allele frequencies lies between the Japanese and North American populations, a divergence to which we shall return later. Genetic diversity does not differ between the Japanese and North American populations, supporting the inferred absence of a founder effect from the history of massive introductions. North American populations are mostly statistically homogeneous, with just a single pairwise F_{ST} being highly significant. Our spatial samples are small in number but encompass the geographic range of self-sustaining naturalized populations in the Pacific Northwest.

The genetic structure of North American populations of the Pacific oyster is typical of the high gene-flow marine species to which 'seascape genetics' has been applied (e.g. Selkoe et al. 2010, 2016, Riginos & Liggins 2013). The majority of such studies are 'link-level' analyses (Wagner & Fortin 2013) that 'focus on pairwise genetic distance and address how seascape features either create discontinuities or promote gene flow between sites' (Selkoe et al. 2016, p. 4)). Typically, a Mantel or partial Mantel test is done to establish correlation between a matrix of pairwise genetic distances, the most frequent response variable (see Table 1 in Riginos & Liggins 2013), and one or more matrices of distance or environmental measures. However, inference of genetic connectivity or gene flow from a single snapshot of pairwise genetic distances relies on the assumption that pairwise genetic distances are near or at equilibrium between migration and drift, at least for neutral markers (Selkoe et al. 2016). Node-level analyses, which focus on associations of allelic richness, heterozygosity, or local F_{ST} (Foll & Gaggiotti 2006) with environmental measures, such as temperature, depth, salinity, and precipitation, must first factor out the geographic component of spatial genetic structure (again, assuming migration-drift equilibrium) and then assume that the response variables are in selection-migration equilibrium. Moreover, alternative approaches in landscape (and seascape) genetics, such as Bayesian clustering or assignment, depend on Hardy-Weinberg and linkage equilibrium in each population (Manel et al. 2003).

The assumptions of linkage and migration-drift equilibria fail spectacularly for Pacific oysters in North

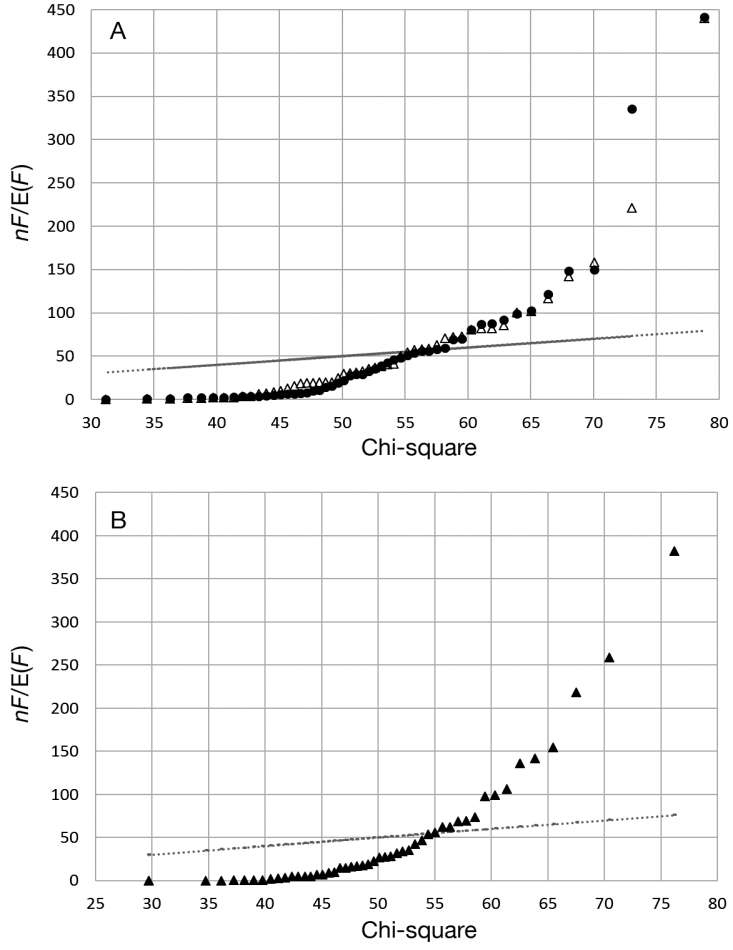

Fig. 4. (A) Probability plot of transformed temporal F_s statistics, $n\tilde{F}/\bar{F}$ for the Dabob Bay (△) and Pipestem Inlet (●) populations (*y*-axis, see 'Materials and methods'), against expected inverse chi-squared values with 52 degrees of freedom, based on rank (*x*-axis; $P_{(r\text{-}0.5)/52)}$), with a 1-to-1 chi-squared plot shown for comparison. (B) Plot as in (A), but with data from generations 90 and 100 in a computer simulation of random genetic drift for 50 single nucleotide polymorphisms (SNPs) in a local population of size, $N_e = 100$, $N_e m = 10$, and metapopulation of $N_e = 1000$

America. In 9 of 10 locations, we found significant departures from linkage equilibrium. In 2 locations re-sampled after 5 to 10 generations, significant temporal genetic change was observed. A significant spatial difference between Pipestem Inlet and Dabob Bay in 1990 was erased 20 yr later. Evidently, spatial genetic structure of North American populations of the Pacific oyster is dynamically determined by evolutionary forces that are not in equilibrium.

Our results and the caution that they raise for seascape analysis may well be general for marine species with 'periodic' life histories, which Winemiller (2005) characterized as having high fecundity, planktonic larval dispersal, high early mortality, delayed reproduction, and long adult life. We recommend testing assumptions of Hardy-Weinberg and migration-drift equilibria before conducting a seascape genetics analysis on marine species with periodic life histories. This is not an impossibly high bar to set. Although temporal studies can require decades in order for the signal of random genetic drift to rise above sampling noise (Waples & Do 2010), other indirect genetic methods (1-sample estimates of N_e based on LD) and direct methods (assessing parentage and kinship), which do not depend on the assumption of temporally stable population structure, provide powerful alternative tools for testing equilibrium states (D'Aloia et al. 2013). Combinations of methods, as applied in this study and elsewhere (Hedgecock et al. 2007b, Christie et al. 2010), provide complementary evidence on temporal stability of spatial genetic structure.

Allowing for non-equilibrium spatial genetic structure does not negate the importance of habitat continuity, oceanographic distance, and life history traits in shaping spatial genetic structure (Selkoe et al. 2014). Seascape analyses of high gene-flow species must simply account for the relative contributions and potential confounding of temporal and spatial factors (Selkoe et al. 2016). F_{ST} is affected not only by selection and by gene flow and drift, as captured in Wright's formula, but also by reproduction in species with skewed offspring numbers (Eldon & Wakeley 2009). In other words, reproduction must be added to distance and environment as independent variables in seascape analyses. The environmental factors underlying skewed offspring numbers are extremely important targets for seascape genetics, notwithstanding the challenges posed by direct study of dispersing larval stages and their environments. On the other hand, certain spatial genetic structures, i.e. strong patterns of isolation by distance or genetic discontinuities at basin scales (e.g. Saha et al. 2015)—cases in which global F_{ST} is high, dispersal is limited, physical barriers to dispersal are present, or physical or habitat distances between sampling locations are large—are likely to remain conducive to seascape genetics analysis.

Causes of temporal genetic change and finite N_e estimates

We found average allele-frequency variances, ranging from $F_s = 0.013$ to 0.05 in the 2 series of temporal

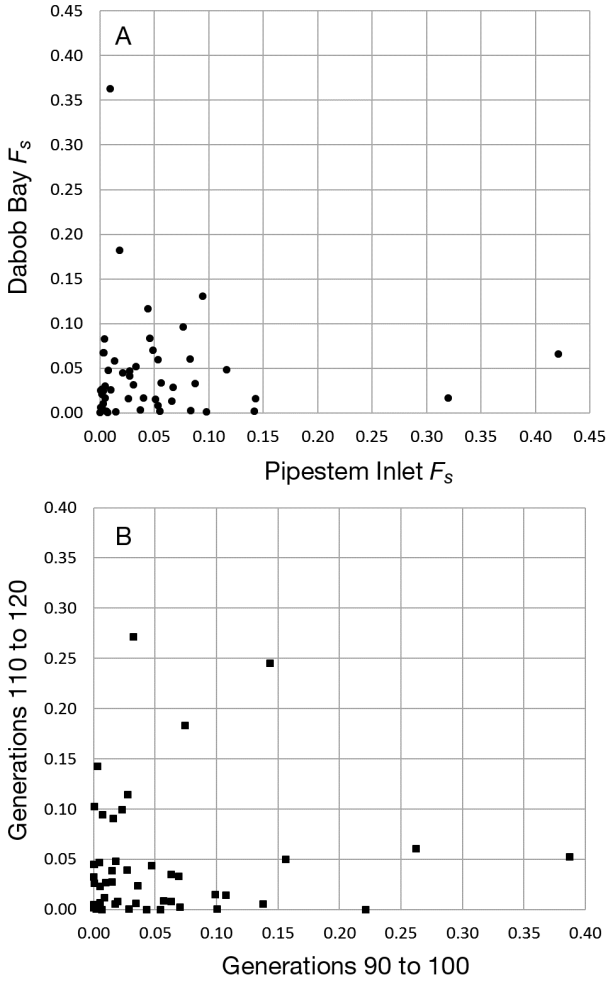

Fig. 5. (A) Locus-specific F_s values in Dabob Bay vs. those in Pipestem Inlet. (B) As in (A), but with data from 2 non-overlapping, 10-generation intervals of random genetic drift in a finite local population with migration from a larger metapopulation (as in Fig. 4)

samples from Pipestem Inlet and Dabob Bay. Temporal genetic variance, put on the same scale as F_{ST}, can be as large as or larger than spatial genetic variance per generation. These estimates of temporal variance imply effective population sizes ranging from ~10^2 to ~10^3, with finite upper confidence limits, far smaller than natural abundance (Quayle 1988, Hedgecock 1994). These findings are in substantial agreement with an earlier estimate of $N_e \approx 400$ for Dabob Bay (Hedgecock 1994). The number of adult oysters harvested per year from Dabob Bay was reported to be on the order of 10^7 or 10^8 at that time, at least 4 to 6 orders of magnitude more than estimated N_e.

The temporal method assumes that (1) populations are closed, (2) generations are discreet, and (3) genetic markers are not directly or indirectly affected by natural selection. The first assumption is obviously violated, since populations of marine species with dispersing planktonic larvae and F_{ST} values approaching 0 are far from closed (Hedgecock et al. 2007a). However, immigration from genetically very similar source populations cannot explain the accumulation of genetic change over time within local populations. For immigration to account for the uncorrelated temporal changes in Pipestem Inlet and Dabob Bay, there would have to exist 2 separate, highly divergent, source populations to drive these changes. Such divergent source populations are implausible, given the great similarity of the populations that we have sampled. Migration should retard, not cause, temporal change in these populations.

When we jointly estimate N_e and m, we obtain very high estimates of m and smaller estimates for local population size, $N_e \approx 10^2$, than the N_e estimates obtained from the traditional temporal method. In other words, for a given amount of temporal genetic variance, local populations under the homogenizing pressure of high gene flow must be smaller than populations that are completely isolated (Gilbert & Whitlock 2015). Temporal estimates of N_e that assume no migration, when migration is actually high, reflect the effective size of the metapopulation (Gilbert & Whitlock 2015), which thus appears to be a surprisingly modest ~10^3. Ryman et al. (2014) noted that temporal estimates of local N_e have a downward bias that approaches 50%, as $m \rightarrow 1$ (panmixia), as inferred here (Table 5). This bias is not nearly large enough, however, to account for the apparent discrepancy between global N_e and natural abundance. Similar observations have been reported by He et al. (2012) for the eastern oyster in Delaware Bay, where the census population on just the New Jersey portion of the bay was estimated to be 1.6×10^9 (Hofmann et al. 2009), while N_e estimates from temporal methods were ~10^2 to ~10^3, albeit with substantial variation and infinite upper bounds in some comparisons.

The second assumption of discrete generations is also violated by 'periodic' marine species, such as the Pacific oyster, which have overlapping generations. Applying the temporal method to populations with overlapping generations can result in biased estimates of N_e (Waples & Yokota 2007), because of increased sampling error on estimates of allelic frequencies. However, this sampling error is constant, whereas drift variance accumulates with time, such that estimates made over intervals of 3 to 5 generations show little bias (Waples & Yokota 2007). The intervals in our study are in this range or higher, so it is unlikely that our estimates suffer from the bias

introduced by overlapping generations. Intervals of this length are also ideal for the ML joint estimates of N_e and m (Wang & Whitlock 2003).

The third major assumption in estimating effective population size from temporal changes in allelic frequencies is that genetic markers are not affected by selection. Analyses of the distributions of temporal genetic variance, F_s, across markers, in actual and simulated populations (Fig. 4), suggest that temporal genetic changes in the Pipestem Inlet and Dabob Bay populations are consistent with random genetic drift and high gene flow. There is no need to invoke selection as an explanation either for the majority of markers showing very small changes over time or for the minority showing large changes. Lack of rank order correlation of locus-specific variances in the 2 temporal series (Fig. 5A) and absence of consistent outliers, together rule out locus-specific diversifying selection as a cause of temporal change. Notably, the selection diversifying Japanese and North American populations for loci on linkage groups 1 and 8 is absent within North America. Thus, temporal genetic variation in these populations is parsimoniously attributed to random drift in allelic frequencies rather than to local adaptation (see below).

Causes of departures from Hardy-Weinberg equilibria and finite N_e estimates

Pacific oyster populations have widespread, though small departures from genotypic proportions expected under random mating at single loci. The global excess of heterozygotes (F_{IS} = −0.0213) is unprecedented, since heterozygote deficiencies have been widely reported for bivalve mollusks and other marine invertebrates (Pacific oyster: Fujio 1979; other oyster species: Hedgecock et al. 2007b; other bivalve mollusks: David et al. 1997). Null alleles are the main cause for deficiencies of heterozygotes at allozyme and microsatellite DNA markers but are rare in HRM assays of SNPs in coding sequences (Sun et al. 2015). Overdominance or associative overdominance can also cause excesses of heterozygotes. Associative overdominance is compatible with evidence for frequent frameshift mutations in the oyster genome (Zhang et al. 2012) and with experiments demonstrating a very high load of deleterious mutations (Plough et al. 2016). In either case, these types of within-family selection would not likely be a problem for seascape analysis. On the other hand, excess heterozygosity may arise when finite pools of male and female parents produce progeny (Hedgecock et al. 2007b), which appears to be the explanation for the Dabob Bay cohort of juveniles with its estimated number of 8 parents.

Pacific oyster populations also depart significantly from linkage or gametic-phase equilibrium. We found significant LD in 9 of 10 population samples, including the native Japanese population, and LD was large enough to support finite, single-sample estimates of N_e in 5 samples from 3 populations (Table 3). These single-sample estimates are in accord with temporal estimates of finite N_e in Pipestem Inlet and Dabob Bay, although they pertain to different time intervals. The LD method also revealed a finite N_e of 132 for another location, Hisnet Inlet, for which we have no temporal data.

Again, we consider the assumptions behind these single-sample estimates of effective population size. First, linkage of HRM markers does not cause or inflate the average LD; unlinked pairs of markers provide 87% (1148/1326) of the observations, and average LD is the same for linked and unlinked pairs of markers (Table S1 in Supplement 1). Second, global epistatic selection seems highly implausible as a cause of LD, since different pairs of markers contribute to LD in different populations (Tables S2 & S3 in Supplement 1). Finally, a statistical partitioning of variance in LD among pairs of loci shows that 99% of the variance is within rather than among populations, implying absence of consistent epistatic selection for particular di-genic combinations (Ohta 1982).

Migration among genetically similar populations cannot produce admixture LD and should instead retard local drift variance, leading to an upward bias in estimates of local N_e (Waples & England 2011). Indeed, with high migration rates, as estimated above, local estimates of N_e converge on an estimate of global N_e (Waples & England 2011). Global N_e estimates from temporal and LD methods are in reasonable agreement, despite a downward bias in the former (Ryman et al. 2014) and an upward bias in the latter.

Our observations of temporal genetic change and LD cannot be explained by global forms of selection, but might they be consistent with local adaptation? Local adaptation is evolutionarily implausible, however, because natural selection should favor generalist strategies in the face of environmental variation that is fine-grained with respect to the dispersal of planktonic larvae from parental habitats (Levins 1968). One such generalist strategy is indeed revealed by the sequence of the Pacific oyster genome, which shows tremendous expansions of gene families asso-

ciated with physiological resilience to environmental stresses (Zhang et al. 2012). For example, the Pacific oyster has 88 genes coding for heat shock protein 70 and 48 genes coding for apoptosis-inhibitor proteins, compared to ~17 and 8 genes, respectively, in the human genome. Each oyster thus carries tremendous genetic and biochemical diversity to cope with changing environments, obviating the cost of selection were this diversity maintained as genetic polymorphisms. By requiring a complex set of ad hoc hypotheses to explain the observations, local adaptation appears vulnerable to Occam's Razor, particularly when a simpler explanation exists, as follows.

Sweepstakes reproductive success

The departures from linkage and migration-drift equilibria that we observe for the Pacific oyster in North America are most parsimoniously attributable to random genetic drift. The evidence from temporal and single-sample methods of analysis implies that North American populations of the Pacific oyster are a highly connected metapopulation with an effective size on the order of ~10^3. This metapopulation comprises local demes that independently and sporadically experience high rates of random genetic drift, owing to small effective population sizes on the order of ~10^2. These estimates of effective population size appear to be several orders of magnitude smaller than the natural abundance of Pacific oysters in the Pacific Northwest, a set of facts consistent with the hypothesis of sweepstakes reproductive success in highly fecund organisms (Hedgecock & Pudovkin 2011), as are observations of significant LD even among unlinked loci (Eldon & Wakeley 2008). Sweepstakes reproduction likely arises from frequent mismatches between the reproductive activity of adults and the narrow windows of oceanographic conditions conducive to successful spawning, fertilization, larval survival and development, and recruitment. Our results imply that sweepstakes reproduction is a strong, spatially localized feature, not a universal feature seen in all populations at all times, because environmental windows leading to successful recruitment may themselves be spatially heterogeneous, localized or regional (Hedgecock & Pudovkin 2011). As a consequence of these spatially and temporally varying environmental and reproductive processes, many marine species with periodic life histories may have population genetic structures that persist in non-equilibrium states.

Divergence of North American and Japanese populations of Pacific oyster

Most of the spatial variance observed in this study is between the Japanese and North American populations and is concentrated in 2 different genomic locations, where F_{ST} is nearly 10 times higher than background (Fig. 3A,B). Since a founder effect or admixture of diverged source populations can safely be rejected as potential explanations (Supplement 1), diversifying natural selection is the most likely explanation. Here, a seascape analysis appears warranted. The coast of North America has relatively colder summer ocean waters than that of Japan, so introduced *Crasssostrea gigas* could have experienced strong selection for adaptation to colder waters and potentially shorter reproductive seasons (Quayle 1988, Boom et al. 1994). Whole-genome scans could shed light on how natural selection has shaped divergence of North American from Japanese Pacific oysters.

Acknowledgements. We thank the program of China Scholarships Council (CSC, 2011633030) for financial support of X.S. Dr. Andrew Beckenbach kindly provided the 1990 samples from British Columbia. We thank Dr. Gordon Liukart for the suggestion to use SimuPOP and especially Dr. Tiago Antão for writing the SimuPOP code. We thank Dr. Robin Waples for constructive criticisms and contributions to an earlier draft. This work was supported by the Paxson H. Offield Professorship in Fisheries Ecology and is dedicated to the memory of Paxson H. Offield, who passed away on 14 June 2015.

LITERATURE CITED

Belkhir K, Borsa P, Chikhi L, Raufaste N, Bonhomme F (2004) GENETIX 4.05.2, logiciel sous Windows TM pour la génétique des populations. Laboratoire Génome, Populations, Interactions, Université de Montpellier II, Montpellier. Available at www.genetix.univ-montp2.fr/genetix/genetix.htm

Boom JDG, Boulding EG, Beckenbach AT (1994) Mitochondrial DNA variation in introduced populations of Pacific oyster, C*rassostrea gigas*, in British Columbia. Can J Fish Aquat Sci 51:1608–1614

Christie MR, Johnson DW, Stallings CD, Hixon MA (2010) Self-recruitment and sweepstakes reproduction amid extensive gene flow in a coral-reef fish. Mol Ecol 19: 1042–1057

Cowen RK, Sponaugle S (2009) Larval dispersal and marine population connectivity. Annu Rev Mar Sci 1:443–466

D'Aloia CC, Bogdanowicz SM, Majoris JE, Harrison RG, Buston PM (2013) Self-recruitment in a Caribbean reef fish: a method for approximating dispersal kernels accounting for seascape. Mol Ecol 22:2563–2572

David P, Perdieu MA, Pernot AF, Jarne P (1997) Fine-grained spatial and temporal population genetic struc-

ture in the marine bivalve *Spisula ovalis*. Evolution 51: 1318–1322

Do C, Waples RS, Peel D, Macbeth GM, Tillett BJ, Ovenden JR (2014) NeEstimator v2: re-implementation of software for the estimation of contemporary effective population size (N_e) from genetic data. Mol Ecol Resour 14:209–214

Eldon B, Wakeley J (2008) Linkage disequilibrium under a skewed offspring distribution among individuals in a population. Genetics 178:1517–1532

Eldon B, Wakeley J (2009) Coalescence times and F_{ST} under a skewed offspring distribution among individuals in a population. Genetics 181:615–629

Excoffier L, Hofer T, Foll M (2009) Detecting loci under selection in a hierarchically structured population. Heredity 103:285–298

Faurby S, Barber PH (2012) Theoretical limits to the correlation between pelagic larval duration and population genetic structure. Mol Ecol 21:3419–3432

Foll M, Gaggiotti O (2006) Identifying the environmental factors that determine the genetic structure of populations. Genetics 174:875–891

Fujio Y (1979) Enzyme polymorphism and population structure of the Pacific oyster, *Crassostrea gigas.* Tohoku J Agric Res 30:32–42

Gilbert KJ, Whitlock MC (2015) Evaluating methods for estimating local effective population size with and without migration. Evolution 69:2154–2166

Goudet J (1995) FSTAT (Version 1.2): a computer program to calculate *F*-statistics. J Hered 86:485–486

Hauser L, Carvalho GR (2008) Paradigm shifts in marine fisheries genetics: ugly hypotheses slain by beautiful facts. Fish Fish 9:333–362

He Y, Ford SE, Bushek D, Powell EN, Bao ZM, Guo XM (2012) Effective population sizes of eastern oyster *Crassostrea virginica* (Gmelin) populations in Delaware Bay, USA. J Mar Res 70:357–379

Hedgecock D (1994) Does variance in reproductive success limit effective population sizes of marine organisms? In: Beaumont AR (ed) Genetics and evolution of aquatic organisms. Chapman & Hall, London, p 122–134

Hedgecock D, Pudovkin AI (2011) Sweepstakes reproductive success in highly fecund marine fish and shellfish: a review and commentary. Bull Mar Sci 87:971–1002

Hedgecock D, Li G, Hubert S, Bucklin K, Ribes V (2004) Widespread null alleles and poor cross-species amplification of microsatellite DNA loci cloned from the Pacific oyster (*Crassostrea gigas*). J Shellfish Res 23:379–385

Hedgecock D, Barber P, Edmands S (2007a) Genetic approaches to measuring connectivity. Oceanography 20:70–79

Hedgecock D, Launey S, Pudovkin AI, Naciri Y, Lapegue S, Bonhomme F (2007b) Small effective number of parents (N_b) inferred for a naturally spawned cohort of juvenile European flat oysters *Ostrea edulis.* Mar Biol 150: 1173–1182

Hedgecock D, Shin G, Gracey AY, Van Den Berg D, Samanta MP (2015) Second-generation linkage maps for the Pacific oyster *Crassostrea gigas* reveal errors in assembly of genome scaffolds. G3 Genes Genomes Genet 5:2007–2019

Hedrick PW (2005) A standardized genetic differentiation measure. Evolution 59:1633–1638

Hofmann E, Bushek D, Ford S, Haidvogel D and others (2009) Understanding how disease and environment combine to structure resistance in estuarine bivalve populations. Oceanography 22:212–231

Jorde PE, Ryman N (2007) Unbiased estimator for genetic drift and effective population size. Genetics 177:927–935

Langdon C, Evans F, Jacobson D, Blouin M (2003) Yields of cultured Pacific oysters *Crassostrea gigas* Thunberg improved after one generation of selection. Aquaculture 220:227–244

Levins R (1968) Evolution in changing environments. Princeton University Press, Princeton, NJ

Manel S, Holderegger R (2013) Ten years of landscape genetics. Trends Ecol Evol 28:614–621

Manel S, Schwartz M, Luikart G, Taberlet P (2003) Landscape genetics: combining landscape ecology and population genetics. Trends Ecol Evol 18:189–197

Mann R (1979) Exotic species in mariculture. Massachusetts Institute of Technology, Cambridge, MA

Nei M (1978) Estimation of average heterozygosity and genetic distance from a small number of individuals. Genetics 89:583–590

Nei M, Tajima F (1981) Genetic drift and estimation of effective population size. Genetics 98:625–640

Nomura T (2008) Estimation of effective number of breeders from molecular coancestry of single cohort samples. Evol Appl 1:462–474

Ohta T (1982) Linkage disequilibrium due to random genetic drift in finite subdivided populations. Proc Natl Acad Sci USA 79:1940–1944

Peakall R, Smouse PE (2012) GenAlEx 6.5: genetic analysis in Excel. Population genetic software for teaching and research. Bioinformatics 28:2537–2539

Peng B, Kimmel M (2005) simuPOP: a forward-time population genetics simulation environment. Bioinformatics 21: 3686–3687

Plough LV, Shin G, Hedgecock D (2016) Genetic inviability is a major driver of type-III survivorship in experimental families of a highly fecund marine bivalve. Mol Ecol 25: 895–910

Pollak E (1983) A new method for estimating the effective population size from allele frequency changes. Genetics 104:531–548

Quayle DB (1988) Pacific oyster culture in British Columbia. Canadian Bulletin of Fisheries and Aquatic Sciences No. 218. Department of Fisheries and Oceans, Ottawa, ON

Raymond M, Rousset F (1995) GENEPOP (version 1.2): population genetics software for exact tests and ecumenicism. J Hered 86:248–249

Rice WR (1989) Analyzing tables of statistical tests. Evolution 43:223–225

Riginos C, Liggins L (2013) Seascape genetics: populations, individuals, and genes marooned and adrift. Geogr Compass 7:197–216

Rousset F (2008) Genepop '007: a complete re-implementation of the GENEPOP software for Windows and Linux. Mol Ecol Resour 8:103–106

Ryman N, Allendorf FW, Jorde PE, Laikre L, Hossjer O (2014) Samples from subdivided populations yield biased estimates of effective size that overestimate the rate of loss of genetic variation. Mol Ecol Resour 14:87–99

Saha A, Hauser L, Kent M, Planque B and others (2015) Seascape genetics of saithe (*Pollachius virens*) across the North Atlantic using single nucleotide polymorphisms. ICES J Mar Sci 72:2732–2741

Selkoe KA, Gaggiotti OE, Bowen BW, Toonen RJ (2014) Emergent patterns of population genetic structure for a coral reef community. Mol Ecol 23:3064–3079

Selkoe KA, D'Aloia CC, Crandall ED, Iacchei M and others (2016) A decade of seascape genetics: contributions to basic and applied marine connectivity. Mar Ecol Prog Ser 554:1–19

Sun X, Shin G, Hedgecock D (2015) Inheritance of high-resolution melting profiles in assays targeting single nucleotide polymorphisms in protein-coding sequences of the Pacific oyster *Crassostrea gigas*: implications for parentage assignment of experimental and commercial broodstocks. Aquaculture 437:127–139

Wagner HH, Fortin MJ (2013) A conceptual framework for the spatial analysis of landscape genetic data. Conserv Genet 14:253–261

Wang J (2001) A pseudo-likelihood method for estimating effective population size from temporally spaced samples. Genet Res 78:243–257

Wang J, Whitlock MC (2003) Estimating effective population size and migration rates from genetic samples over space and time. Genetics 163:429–446

Waples RS (1989) A generalized approach for estimating effective population size from temporal changes in allele frequency. Genetics 121:379–391

Waples RS (1998) Separating the wheat from the chaff: patterns of genetic differentiation in high gene flow species. J Hered 89:438–450

Waples RS, Do C (2008) LDNE: a program for estimating effective population size from data on linkage disequilibrium. Mol Ecol Resour 8:753–756

Waples RS, Do C (2010) Linkage disequilibrium estimates of contemporary N_e using highly variable genetic markers: a largely untapped resource for applied conservation and evolution. Evol Appl 3:244–262

Waples RS, England PR (2011) Estimating contemporary effective population size on the basis of linkage disequilibrium in the face of migration. Genetics 189:633–644

Waples RS, Yokota M (2007) Temporal estimates of effective population size in species with overlapping generations. Genetics 175:219–233

Waples RS, Antao T, Luikart G (2014) Effects of overlapping generations on linkage disequilibrium estimates of effective population size. Genetics 197:769–780

Weir BS, Cockerham CC (1984) Estimating *F*-statistics for the analysis of population structure. Evolution 38: 1358–1370

Whitlock MC, McCauley DE (1999) Indirect measures of gene flow and migration: $F_{ST} \neq 1/(4Nm+1)$. Heredity 82: 117–125

Winemiller KO (2005) Life history strategies, population regulation, and implications for fisheries management. Can J Fish Aquat Sci 62:872–885

Wright S (1931) Evolution in Mendelian populations. Genetics 16:97–159

Zhang G, Fang X, Guo X, Li L and others (2012) The oyster genome reveals stress adaptation and complexity of shell formation. Nature 490:49–54

Zhdanova OL, Pudovkin AI (2008) Nb_HetEx: a program to estimate the effective number of breeders. J Hered 99: 694–695

Editorial responsibility: Philippe Borsa, Montpellier, France

Submitted: July 28, 2016; Accepted: December 11, 2016
Proofs received from author(s): February 1, 2017